Density-functional calculation of methane adsorption on graphite (0001)

Shizhong Yang, Lizhi Ouyang, James M. Phillips, and W. Y. Ching
Physics Department, University of Missouri-Kansas City, Kansas City, Missouri 64110, USA
(Received 20 July 2005; revised manuscript received 9 January 2006; published 12 April 2006)

Methane adsorbed on graphite was studied using density-functional theory. The structure was fully optimized with strict energy and force convergence criteria. The methane converged to the preferred adsorption sites giving the vibrational frequencies, the energy of adsorption, charge distributions, and the electronic density of states. Under the two coverages studied ($\sqrt{3}\times\sqrt{3}$ and $2\sqrt{3}\times 2\sqrt{3}$) and a differing number of graphite layers (1–6), the methane molecules favored atop sites on the graphite surface with the hydrogen tripod down. We found the methane carbon 3.21 Å above the graphite carbon and the adsorption energy to be 118 meV for the lower coverage. The independent harmonic oscillator vibrational frequency perpendicular to the surface for the CH_4 molecule was computed to be 87 cm^{-1}. The graphite surface contracted 5.0% and 4.1% for the first and second layers, respectively, from the spacing relative to their bulk values. To benchmark our frequency calculations, we also used second-order Moller-Plesset theory and the local spin density approximation (LSDA) in GAUSSIAN 03 for the molecule. All of our LDA results are in good agreement with corresponding experiments, while under the generalized gradient approximation approximation we get only qualitatively results.

DOI: 10.1103/PhysRevB.73.165407 PACS number(s): 68.43.Bc, 68.43.Fg, 68.43.Pq, 68.47.De

I. INTRODUCTION

In this study, we calculate the properties of CH_4 adsorbed on graphite by using a first-principles density functional theory (DFT) and applying periodic boundary conditions. Investigations of this system have been among the more important ones in the early development of two-dimensional matter. Until recently, a fully quantum mechanical treatment of the CH_4/graphite system seemed beyond our reach. This paper is a continuation of earlier classical calculations[1–6] which we have now extended by employing a fully quantum mechanical method. We have approached the problem in two ways, one with quantum chemical calculations[7] and, more completely, with first-principles DFT employing the electronic band structures of the periodic complex.[8–13]

The study of methane adsorbed on graphite has a rich history for both its practical and theoretical importance. Reviews have been written by Bruch *et al.*,[14] Vidali,[15] Dash,[16] and earlier by Steele.[17] A number of heat capacity experiments,[18–24] adsorption isotherms,[25,26] NMR studies,[27–29] neutron scattering investigations,[30–38] and low-energy electron diffraction[39] led to important quantitative understanding of the behavior of adsorbates. In earlier computations, empirical atom-atom potentials were developed[1–6,40–42] and lattice dynamics methods[41,42] were employed, and computer simulations[43,44] have been applied to CH_4/graphite adsorption. Since methane forms a $\sqrt{3}\times\sqrt{3}$ registered structure, it became a test system for commensurate-incommensurate transitions.[1–6,45]

Recently, CH_4 on carbon nanotubes have proved to be very topical in the area of nanotechnology. Both methane molecules[46,47] and graphite nanotubes[48–53] are closely related to several applications. For example, it is necessary to know the adsorption energy and other properties in order to devise an optimum capability of methane gas storage by adsorption on graphite materials.

Our paper is organized in the following manner. Section 1 is an introduction, Sec. II is a description of our computational methods for the VASP calculations. Section III reports the results for bulk graphite (Sec. III A) and the methane molecule (Sec. III B). Our results for the structure and adsorption energy are given for the adsorption of methane on graphite (Sec. III C). In Sec. III D, we present our results for the electronic structure of the adsorption complex, and Sec. III E gives our results for frequencies for adsorbed methane on graphite. Section IV contains our discussion and conclusions. We have separated out our GAUSSIAN calculations in the Appendix.

II. COMPUTATIONAL METHODS

Our primary calculation method uses the Vienna *ab inito* simulation package (VASP),[8–13] applied to a periodic adsorbate and substrate complex for the CH_4/graphite model. We also used GAUSSIAN 03 with periodic boundary conditions[7] on a model with only one layer of graphite as a cross check to the values computed by VASP (see the Appendix).

We employed a plane-wave basis set and the projection-augmented-wave (PAW) method rather than the ultrasoft pseudopotentials for the carbon and hydrogen atoms of our system. Both the local density approximation (LDA) and generalized gradient approximation (GGA) for the local and gradient-corrected correlation functionals were used when the computational package allowed. In the VASP approach, the solutions of the generalized self-consistent Kohn-Sham equations are calculated using an efficient matrix-diagonalization routine based on a sequential band-by-band residual minimization method and a Pulay-like charge density mixing.[54] Optimization of the atomic geometries was calculated using the total energies and by minimizing the energy with a quasi-Newton quench using the Hellmann-Feynman forces. In this work, we applied a plane-wave basis cutoff at 500 eV and a fine augmented charge cutoff at 2000 eV. The atom coordinates were fully relaxed in both the adsorbate and the substrate. The relaxation convergence

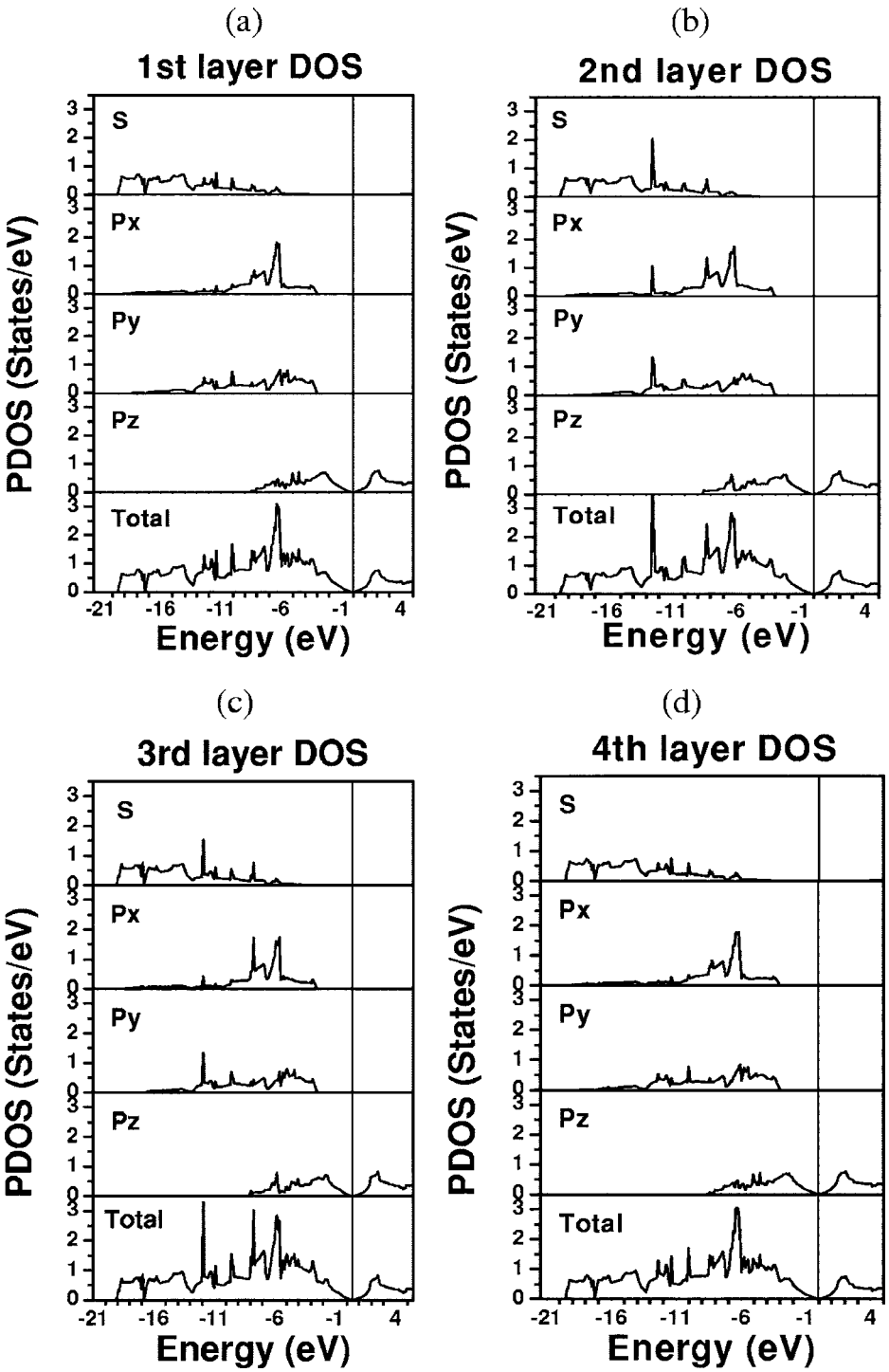

FIG. 1. The electronic DOS graph for the individual four layers of a graphite sheet. The Fermi level that is at 0 eV in each graph is indicated by a solid vertical line.

of the residual force was set at 0.05 meV/Å unless otherwise noted (note, this very fine convergence criterion is required for the later calculation of frequencies[8]). The starting lattice constant values are obtained from the bulk graphite calculation. The Brillouin zone is a $1\times1\times1$ primitive unit cell with four carbon atoms contained inside. It was sampled by a Monkhorst-Pack $12\times12\times6$ k-point grid. The total energy versus plane-wave and k-point convergences were checked to be less than 1 meV. The results from this computation for bulk graphite gave the lattice constants using the PAW and LDA were $a=2.467$ Å and $c=6.925$ Å, which compare well with the experiments.[55–57] The results using the LDA are slightly closer to those of experiment than those using the GGA when comparing lattice constants only. As we shall see in a later section, the comparisons for adsorption energies are quite different; the GGA energies were far from those of a comparable experiment.

Using VASP, we calculated both $\sqrt{3}\times\sqrt{3}$ and $2\sqrt{3}\times2\sqrt{3}$ structures of methane adsorbed on one, two, four, and six layers of graphite. In the $\sqrt{3}\times\sqrt{3}$ cases, each unit cell for a single graphite layer has six carbon atoms (with three carbons on the cell boundary and three carbons in the interior)

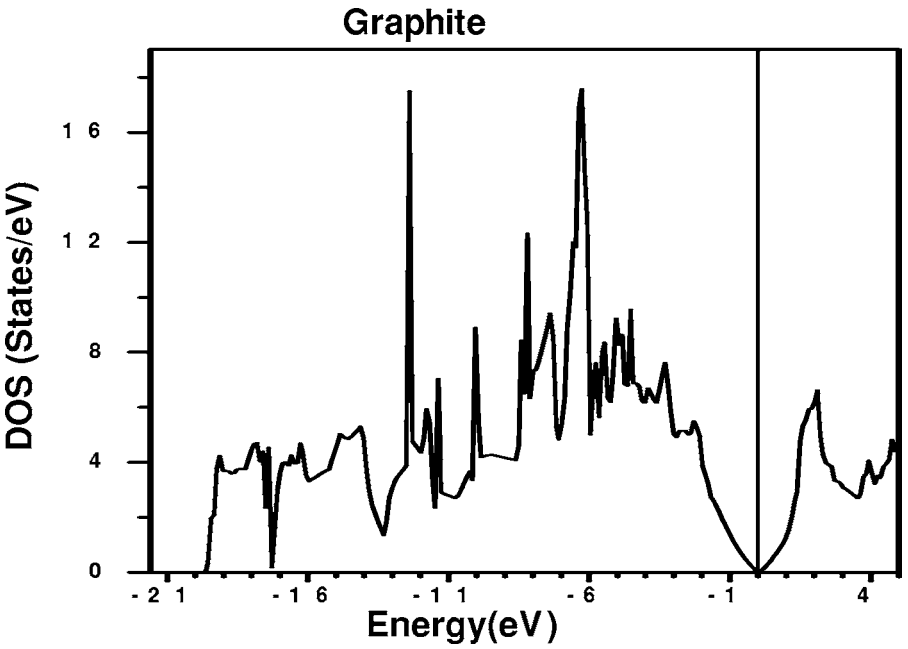

FIG. 2. Total DOS for four layers of graphite.

giving a total of 41 atoms in our largest unit cell (see Fig. 3 below). For the $2\sqrt{3}\times 2\sqrt{3}$ coverage, it has 24 carbon atoms on each layer.

The empty vertical distance for periodic unit cells is 16 Å for one layer, 20 Å for a slab of two layers, and also in the case of four layers. This distance is 30 Å for a six-layer slab unit cell. In these two latter models for the CH_4/graphite system, the Brillouin zone integrations were performed on a grid of $7\times 7\times 1$ Monkhorst-Pack special points. We found reasonable consistency in the computed structure and energies. The structures, adsorption energies, vibrational frequencies, and electronic properties were calculated using DFT under the LDA.

The adsorption energy is taken to be

$$E_{\mathrm{ab}} = E(\mathrm{CH_4/graphite}) - E(\mathrm{graphite}) - E(\mathrm{CH_4}),$$

where $E(\mathrm{CH_4/graphite})$ is the energy of the total system, $E(\mathrm{graphite})$ is the energy of the graphite alone and $E(\mathrm{CH_4})$ is the energy of the isolated (gas phase) CH_4 molecule.

The cluster method (see Refs. 58–60 for reviews) can be used to model adsorption systems like our methane on graphite using an accurate method like second-order Moller-Plesset (MP2) theory or coupled cluster singles and doubles, but the cluster size must be unreasonably small to make the run times practical; however, the frequency computations as a local property are reasonable.[58] Adsorption energies for any cluster model are much too high.[58] The comparison of the advantages and disadvantages of the two methods has been discussed[58] (see the Appendix). Our use of periodic boundary conditions avoids some of these problems and as a result, the calculations are able to achieve some reasonable accuracy with low computational cost. First-principles DFT calculations using plane waves are often the more accurate computational method. For these reasons, we chose the periodic boundary method to calculate the properties for the methane on graphite system. Recent reports on gases adsorbed on graphite nanotubes indicate a current interest in our system.[61–64]

TABLE I. The methane molecule vibrational frequency by MP2, LSDA, and VASP calculations (cm^{-1}). The mode symbols are taken from Ref. 46.

	Gaussian 03			
	MP2 and 6-311G**	LSDA and 6-311G**	VASP	Experiment (Ref. 46)
*F*2	1363.07	1260.36	1250.36	1306.2 (*I* active)
E	1579.37	1490.98	1480.51	1526 (*R* active)
*A*1	3082.07	2974.91	2957.69	2914.2
*F*2	3220.40	3106.86	3082.05	3020.3 (*I* and *R*)

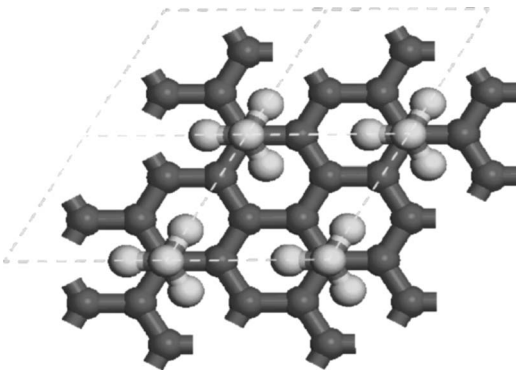

FIG. 3. $\sqrt{3}\times\sqrt{3}$ unit cell (top view) of full coverage of one monolayer of methane on graphite optimized by VASP and G03. The white balls are the hydrogen atoms and the dark gray balls are the carbon atoms. The two-dimensional cell size is 4.239×4.239 Å for VASP and 4.26×4.26 Å for G03. The system has C_{3v} symmetry.

TABLE II. Adsorption energy of methane on graphite (0001) surface (meV).

	GAUSSIAN 03 (GGA)	VASP (LDA)	VASP (GGA)
One layer $(\sqrt{3}\times\sqrt{3})$	147	182	24.3
$(2\sqrt{3}\times 2\sqrt{3})$		122	13.6
Two layer $(\sqrt{3}\times\sqrt{3})$		180	
$(2\sqrt{3}\times 2\sqrt{3})$		118	
Four layer $(\sqrt{3}\times\sqrt{3})$		180	
Six layer $(\sqrt{3}\times\sqrt{3})$		180	
Experiment	126 meV from Ref. 15 "best estimate" at zero coverage		

III. RESULTS AND DISCUSSIONS

A. Bulk graphite

Although bulk graphite has been studied previously,[55,65–69] it is necessary that we begin our adsorption calculations with a VASP calculation of bulk graphite alone. Using the same methods and parameters as the starting calculations, we will then test our model with a four-layer slab of graphite. The optimized structure now provides us with a basis and the starting values for the full adsorption model calculations. We observe the following results for our graphite model. The surface layer-layer distance has contracted to $\Delta d_{12}/d_0=5.0\%$ and $\Delta d_{23}/d_0=4.1\%$ where d_{12} is the distance between the first and second layers and d_0 is the bulk layer-layer distance, i.e., from $d_0=3.463$ Å to $d_{12}=3.29$ Å for our optimized model. Experimentally, it is often difficult to measure the contraction of a surface.

The electronic density of states (DOS) of our four layer slab is given in Fig. 1. From Fig. 1, we can see that the conduction band and the valence band are continuous at the Fermi level but the DOS is zero. Thus, in the normal state, we find graphite to be a semimetal, as one would expect. The DOS in Fig. 1 shows that in parts (a) through (d) the s, p_x, and p_y orbitals are in the same energy range, indicating that the sp^2 hybridization feature still exists in both the surface and internal layers. The surface layers have a similar DOS curve as the inner ones but the surface results have additional electronic states. As can be seen from Fig. 1, the first layer (a) has almost the same profile as the fourth layer (d) while the second layer DOS in (b) is very similar to that of the third layer (c). Comparing our results for the total DOS in Fig. 2 with the earlier calculations,[65,66] and experiments,[70,71] our results show a solid consistency.

B. The structure and vibrational frequencies calculated for the methane molecule

Our next step was to calculate the optimized structure and vibrational frequencies for the methane molecule using the methods and parameters applied to the full adsorption complex. Our results are in reasonable agreement with experimental values.[46,47]

Using VASP, a methane molecule was put in a $15\times 15\times 15$ Å^3 box and was calculated with 500 eV plane-wave cutoff and the k-point sampling only. The residual force convergence value was set to less than 0.02 meV/Å. Also for comparison purposes, we use the quantum chemical package GAUSSIAN G03 and with the perturbation theory approach MP2 and the local spin density approximation (LSDA) using 6-311G** as a basis set (see the Appendix). The results are summarized in Table I.

In addition to the vibrational frequencies, we obtained three frequencies near zero and three very small imaginary frequencies. The very small positive modes are due to the zero-point energy and the imaginary frequencies represent the translational modes. Note further that the two $F2$ modes are threefold degenerate and the E modes are twofold degenerate, giving a total of 15 modes. The bond lengths compare well with each other and to experiment; by G03 LSDA with 6-311G**, the C-H distance is equal to 1.0897 Å using MP2 it is 1.0972 Å. The VASP result was 1.0979 Å and experiment gives 1.0850 Å.[46,47]

C. Adsorption energy and structure of methane on graphite

Two different coverages of methane were studied, $\sqrt{3}\times\sqrt{3}R(30^\circ)$ and $2\sqrt{3}\times 2\sqrt{3}R(30^\circ)$. The second coverage is our attempt to compare to data taken in the low-coverage limit. Our results are listed in the Table II. Experiments by Ross *et al.*,[25,26] and reviewed by Vidali *et al.*[15] gave a value for the energy of adsorption at low coverage to be 126 meV. In the case of one-layer graphite (graphene) for $2\sqrt{3}\times 2\sqrt{3}$ coverage we compute the adsorption energy to be 122.3 meV. For two layers of the graphite substrate, the ad-

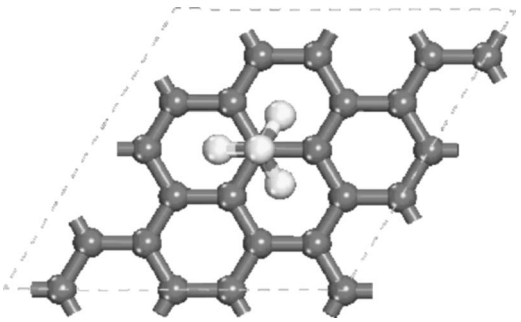

FIG. 4. $2\sqrt{3}\times 2\sqrt{3}$ unit cell (top view) methane molecule on graphite sheet. The white balls are hydrogen atoms and the dark gray balls are carbon atoms.

TABLE III. The VASP LDA optimization results. Distance from methane carbon directly right underneath graphite carbon is $d_{C\text{-}C}$, the distance from the carbon atom to top hydrogen atoms is $d_{C\text{-}H(T)}$, while the distance from the carbon atom to the bottom hydrogen atom is $d_{C\text{-}H(B)}$. Δd is the distance change from indented carbon right under methane carbon to the surface layer. The units are angstroms.

	$d_{C\text{-}C}$	$d_{C\text{-}H(T)}$	$d_{C\text{-}H(B)}$	Δd	$d_{C\text{-}C}$ (VASP GGA)	$d_{C\text{-}C}$ (G03 GGA)
One layer ($\sqrt{3}\times\sqrt{3}$)	3.22	1.10	1.10	0.005	4.10	3.81
($2\sqrt{3}\times 2\sqrt{3}$)	3.22	1.10	1.10	0.019	3.89	
Two layer ($\sqrt{3}\times\sqrt{3}$)	3.22	1.10	1.10	0.006		
($2\sqrt{3}\times 2\sqrt{3}$)	3.26	1.10	1.09	0.009		
Four layer ($\sqrt{3}\times\sqrt{3}$)	3.21	1.10	1.10	0.006		
Six layer ($\sqrt{3}\times\sqrt{3}$)	3.21	1.10	1.10	0.006		
Experiment	(a) $d_{C\text{-}C}$=3.45 from Ref. 15 the "best estimate" at zero coverage (b) $d_{C\text{-}C}$=3.3±0.05 from Refs. 26 and 38 $\sqrt{3}\times\sqrt{3}$ coverage					

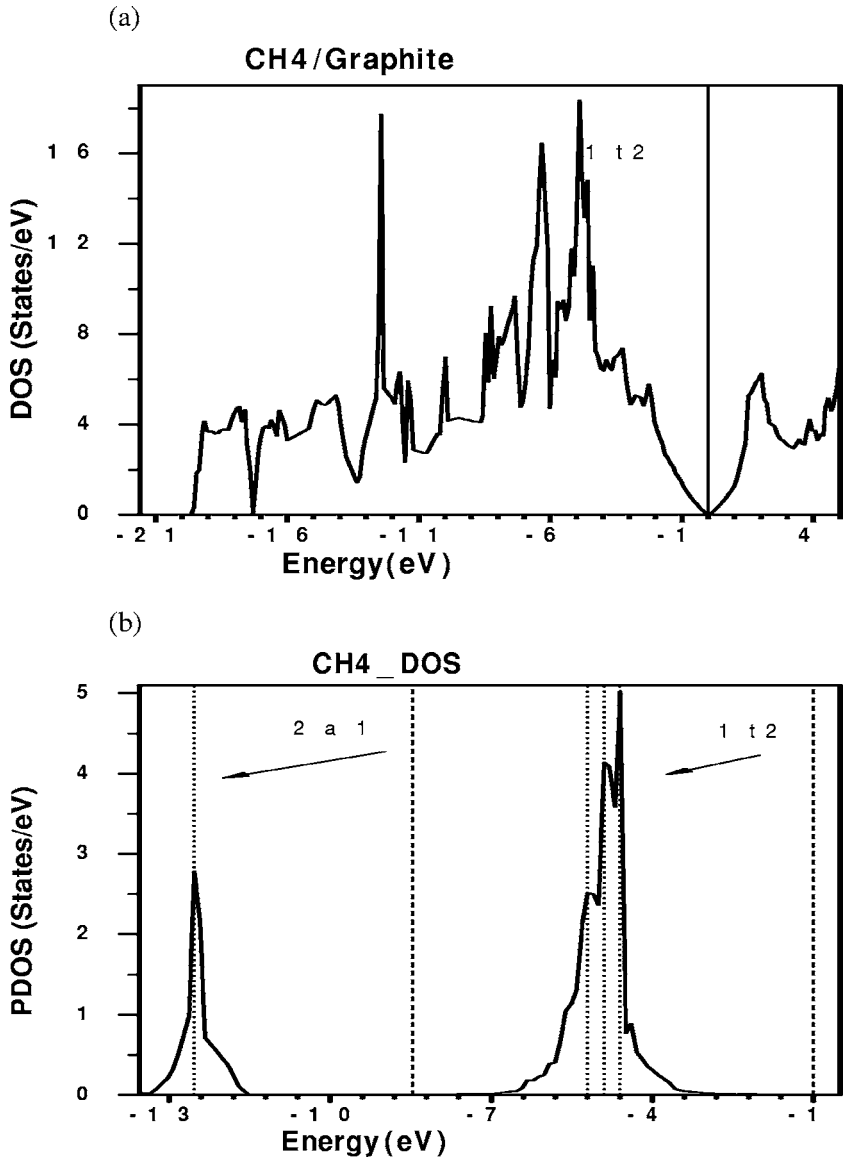

FIG. 5. Total DOS of CH_4/graphite and CH_4 after adsorption. In (b) the dashed lines are the CH_4 gas state molecule energy levels and the dotted ones are the corresponding energy levels after adsorption.

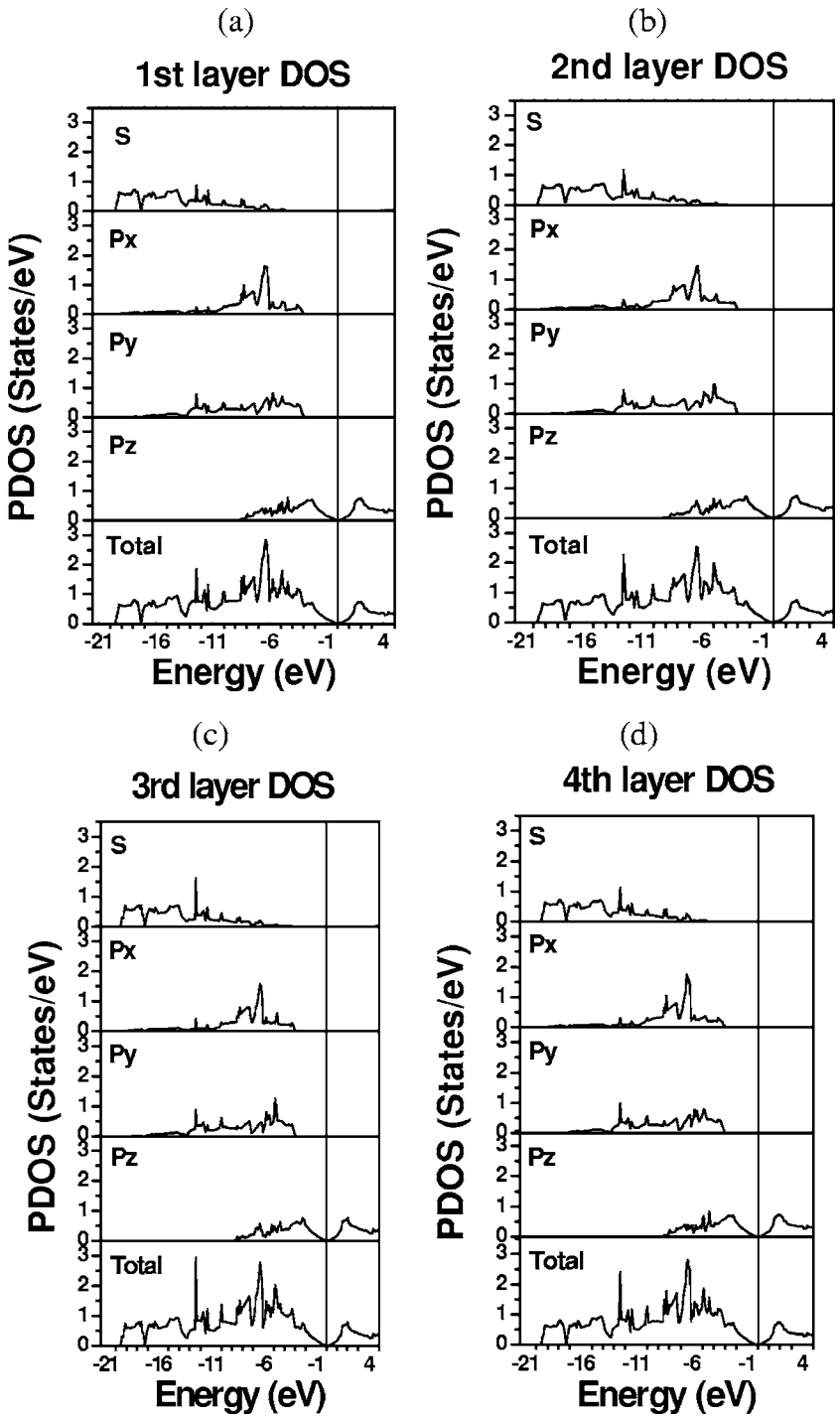

FIG. 6. Partial DOS of graphite by layer after CH_4 adsorption.

sorption energy is found to be 118.07 meV. The repulsion of the hydrogens by the carbons atoms in the second layer appears to lower the adsorption energy. These results are close to their "best estimate" experimental value[15,25] of 126 meV at low coverage. This is less than the corresponding VASP LDA value 182.436 meV. The VASP GGA values are 24.295 and 13.634 meV for one-layer $\sqrt{3}\times\sqrt{3}$ and $2\sqrt{3}\times 2\sqrt{3}$, respectively. Compared with experiment values, our VASP GGA result dramatically underestimates the molecule-surface interaction. It is well known that the GGA in VASP usually gives very small adsorption energy for physisorption systems.[72]

Our model of the CH_4/graphite system has C_{3v} symmetry. All of our calculations were optimized to a stable geometry: the methane carbon is sitting in an atop site of the graphite substrate with the tripod legs oriented toward the centers of three adjacent graphite hexagons (see Figs. 3 and 4). This structure is in agreement with the classical simulation results using the Lennard-Jones 12-6 potential and also with lattice sums applying atom-atom potentials.[1–6,40–42,45]

From Table III, we can see that our calculations give the top C-H bond length changes as very small. In all of our cases we see a trivial elongation of the bottom C-H bond of about 0.001–0.003 Å from the molecule. Our bond length

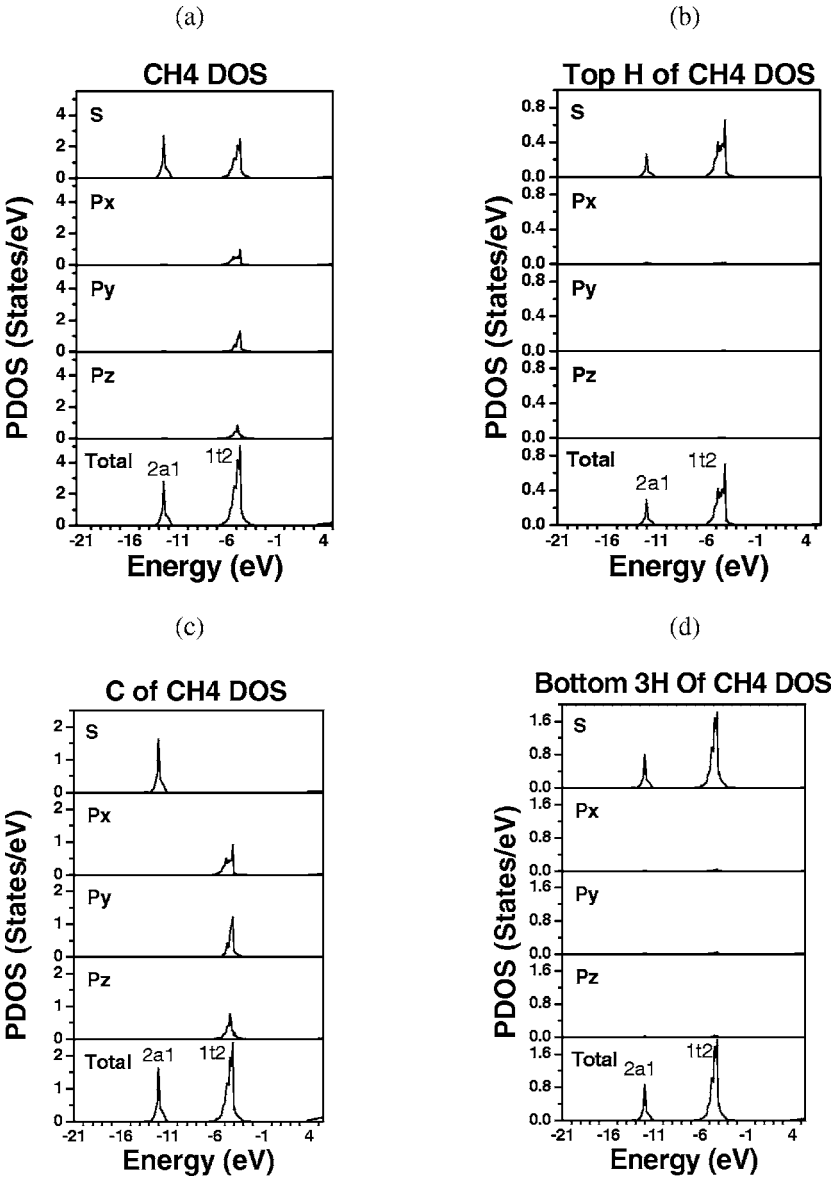

FIG. 7. Partial DOS of the adsorbate CH_4 and its components after adsorption.

results are slightly smaller than the experimental ones. This small difference may due to the overbinding feature of the LDA. For comparison, we calculated the $d_{c\text{-}c}$ value at full coverage with one layer using G03 GGA (the only option available) to be 3.807 89 Å which is somewhat larger than the experimental value. The $d_{\text{C-C}}$ values of VASP GGA are 4.100 10 and 3.892 29 Å for one-layer $\sqrt{3}\times\sqrt{3}$ and $2\sqrt{3}\times 2\sqrt{3}$, respectively, they are also larger than corresponding LDA values. We found using G03 Perdew-Burke-Emzerhof (PBE) with the GGA to give a small overestimation for the bond energy. In the four-layer case, we can see from our VASP optimized results that the carbon atom right under the methane carbon atom contracted into top layer Δd=0.005 62 Å. At $2\sqrt{3}\times 2\sqrt{3}$, the difference is 0.018 83 Å. These values show a sensible trend, but they are well below the computational limits of our model and measurements.

D. Electronic structure of methane on graphite

Earlier, we reported our results for the electronic DOS for the substrate and for the adsorbate. This allows us to note the differences in the electronic structure that occurs upon this particular physical adsorption. We have attempted to show how these earlier values of the pure states are altered in the adsorbed complex.

Figure 5(a) shows the total electronic DOS for the adsorbed complex and Fig. 5(b) plots the DOS of the methane molecule before and after adsorption. It is difficult to distinguish from Fig. 5(a) the contribution of each component since it is the summation DOS of all the components in the system. However, by comparison of Figs. 2 and 5(a), we can clearly see that there is significant change in the DOS near the $1t2$ and $2a1$ peaks. In Fig. 5(b), we compared the energy levels for the gas phase methane molecule. Our results showed that the following molecular energy to be (with reference to the Fermi energy): E_{2a1}=−8.4699 eV, E_{1t2}= −1.0035 eV (triply degenerate), E_{2a1}=8.0024 eV, E_{2t2_1} =8.6416 eV, and E_{2t2_2}=8.9108 eV (doubly degenerate). From Fig. 7 below, we are unable to distinguish the three separated $1t2$ DOS peaks, because the symmetry is not broken, so they are merged. The total DOS near $1t2$ in Fig. 5(b)

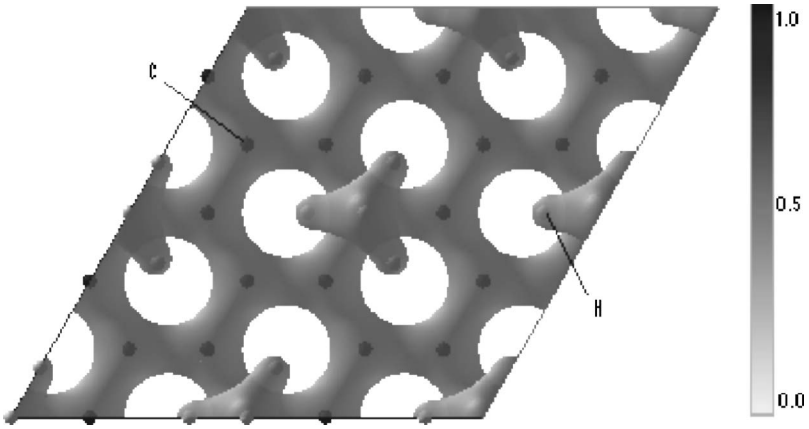

FIG. 8. The top view of the first-layer graphite charge density contours of horizontal *x*-*y* plane for the $\sqrt{3}\times\sqrt{3}$ CH_4/graphite system. The maximum value of 1 is found by 1115 electronic charges divided by the volume of the unit cell.

changes when compared with the same energy levels in this figure from the gas phase molecule. From Fig. 5(b), we can also see that the energy states $E_{2a1}=-12.5281$ eV and the original $1t2$ state separate into three states. From the peak positions $E_{1t2\_h}=-4.5911$ eV, $E_{1t2\_m}=-4.8971$ eV, and $E_{1t2\_l}=-5.2021$ eV we get the energy shift downward to −3.5876 eV, −3.8936 eV, and −3.1986 eV, respectively. These energy shifts combined with the optimized geometry results, suggest that in the CH_4 molecule the $2a1$ and $1t2$ states have interacted with the surface layers of carbon atoms causing a charge redistribution in both CH_4 and in the graphite surface. Thus, in the CH_4 molecule, the bottom three C-H bond lengths have changed slightly while the graphite layer has contracted a small amount.

When comparing Fig. 6 with corresponding parts in Fig. 1, it is relatively hard to distinguish the small changes of those partial DOSs although we can see that the total partial DOS for each layer does increase a small amount near the $1t2$ and $2a1$ energy levels. Figure 7 graphs the DOS for an individual atom upon adsorption. From Fig. 8, we see that the charge density between graphite neighbor carbon atoms is the greatest and at the center of the hexagons is the least. This is consistent with the minimized geometry of the methane. Figure 9 shows that the isodensity of methane molecule has deviated from a nearly spherical shape and the methane density in the graphite side (bottom) is broader than the other three sides of tetrahedron. These figures with their distortions and their optimized minimum are consistent with a rule of thumb in adsorption site selection, "adsorption site selection is a function of steric repulsion."[73]

E. Vibrational frequencies for methane on graphite

Our frequencies for the methane on graphite system are estimated by using the optimized atomic positions and frozen phonon approximation with an assigned virtual displacement. We set this spacing to be 0.05 Å. Then a harmonic oscillator frequency is computed for each vibrational mode. Zero-point contributions are not included. For the methane molecule alone, in Table I we can see that the results using VASP and also with the LSDA in G03 are reasonable when compared to experiment. The results obtained using perturbation theory, MP2 in G03, are also consistent with measurements on methane.

Both $F2$ modes in Table I are triply degenerate. The E mode is doubly degenerate. When the methane molecule is close to the graphite surface, the surface carbon atom right under the methane carbon contracts a small distance, the bottom three H atoms elongate 0.001–0.003 Å, while the original degenerate $F2$ and E modes split into three and two components, respectively. In Table IV, both $F2$ and E modes have redshifted while the second $F2$ mode 3032.3 cm^{-1} has both a red- and a blueshift (See Table IV).

Our VASP calculation of the perpendicular vibrational frequency of the entire methane molecule gave $\omega_\perp=87$ cm^{-1}. This is reasonably close to the phonon data $Q_\perp=100$ cm^{-1} at the zone center[38] which was taken at 70% coverage and in the temperature range from 10 to 70 K. We should note that our frequencies are not phonons. They are the normal mode vibrations of a molecule adsorbed on the graphite surface.

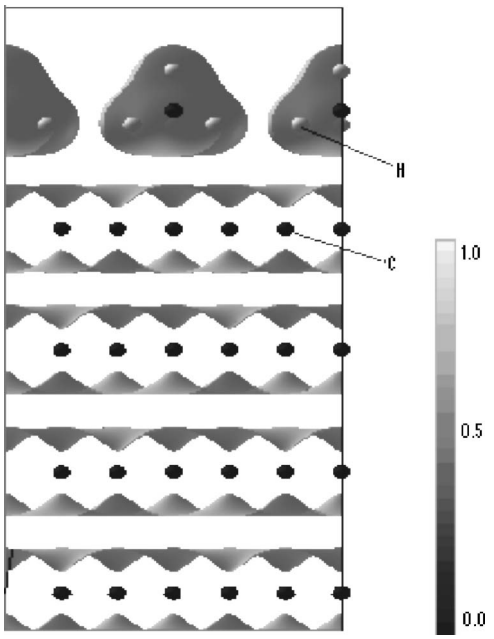

FIG. 9. A side view of the vertical *y*-*z* plane ($x=2.12$ Å) showing the charge density contours of $\sqrt{3}\times\sqrt{3}$ CH_4/graphite. The gray shells around the methane and graphite layers are the isosurface with value 0.05 (relative to maximal value 1.0). The maximum value of one is found by 1115 electronic charges divided by the volume of the unit cell.

TABLE IV. The vibrational frequency of methane on one, two, and four layers of graphite (cm^{-1}). The experimental reference is for CH_4. The shift column represents the value in the four-layer column minus the single-molecule case in Table III VASP column NA indicates not available.

	One layer	Two layer	Four layer	Experiment CH_4 (Ref. 38)	Shift
$\omega_\perp$	84.20	86.59	87.000	100[a]	NA
$\omega_\parallel$	148.66	151.49	149.24	NA	NA
$\omega_\perp$	186.62	195.36	193.30	NA	NA
$F2$ (ν_{3b})	1223.88	1224.53	1224.15	NA	−26.21
$F2$ (ν_{3c})	1242.16	1242.176	1242.29	NA	−8.07
$F2$ (ν_{3a})	1250.36	1250.92	1250.18	NA	−0.18
E (ν_{2b})	1458.02	1458.68	1458.30	NA	−22.21
E (ν_{2a})	1461.29	1461.99	1461.30	NA	−19.21
$A1$ (ν_1)	2931.80	2931.73	2931.65	NA	−26.04
$F2$ (ν_{4a})	3036.26	3036.19	3036.08	NA	−45.97
$F2$ (ν_{4c})	3074.92	3074.76	3074.69	NA	−7.36
$F2$ (ν_{4b})	3094.43	3094.43	3094.69	NA	12.64

[a]Phonon at zone-center (Ref. 38).

These vibrational frequencies are given in Table IV. Some of these are not easily accessible to experiment. $\omega_\parallel$ is the transverse motion of the molecule parallel to the surface is mixed with a δ (HCH) bend. The neutron scattering data have mixed modes for the rotational and tunneling superposition in the phonon spectra.[38] Consequently, the molecular vibrational normal modes in our calculations would not be a valid comparison to the phonon studies other than in the special case of the vertical mode at the zone center.

IV. CONCLUSIONS

Our first-principles DFT method of calculation shows that at zero temperature the methane carbon is sitting on an atop site of the graphite substrate with the tripod legs oriented toward the open centers of three adjacent graphite hexagons. The experimental measurement of the vertical height of the methane carbon above the graphite carbon is 3.3±0.05 Å in Ref. 38. Our VASP LDA result for a monolayer of methane upon graphite is 3.21 Å using six layers of graphite in the unit cell. The top two graphite layers contract 5.0–4.1 % after optimization. In the four-layer case, the carbon atom right under the methane carbon has a contraction of about 0.0056 Å relative to the surface layer while the bottom three C-H bonds elongate by 0.003 Å. These computational results on the layer-to-layer distances are just to demonstrate the computational precision and are far too small to be verified by measurement.

The electronic structure studies show that the methane graphite interaction is mainly occurring via the $2a1$ and $1t2$ states upon adsorption [see Fig. 5(b)]. The $1t2$ state has separated into three states. We were able to predict the frequency shifts of all the vibrational modes. We observe the $F2$, E, and $A1$ modes have redshifts with the largest of these values −26.21, −22.21 and −26.04 cm^{-1}, respectively. The highest $F2$ mode has a blueshift of 12.64 cm^{-1}. We also get lower end frequencies, 186.62 and 148.66 cm^{-1}, that are perpendicular and parallel to the graphite surface, respectively. These higher frequencies are quite different from the neutron scattering data by Bromchil *et al.*,[38] because of two problems: the experimental data have mixed states for rotations and tunneling, and our calculations of the normal modes show internal bending modes within the methane molecule. The independent vertical harmonic vibration frequency of methane molecule is 87 cm^{-1}. The VASP approach gives the correct adsorption site and height, reasonable adsorption energy, and vibrational frequencies. The GGA results of our calculation show that the GGA gives the correct adsorption site but only gives qualitative results for the adsorption energy and the adsorbate heights, which are generally not as good as those in the LDA.[70] We are in good agreement with our earlier work using classical and atom-atom potentials.[1–6]

APPENDIX: A SUMMARY OF OUR QUANTUM CHEMICAL MODEL

For the G03 culations on the methane molecule, we also used the MP2 and LSDA methods in GAUSSIAN 03 with the 6-311** basis set. These were used as an independent check of the frequency values computed by VASP (see Table I).

In order to check the consistency of G03 with VASP, we first optimized a single layer of graphite (graphene) and second optimized the entire complex of CH_4 adsorbed on a $\sqrt{3}\times\sqrt{3}$ unit with only one layer of graphite in our periodic cell. The vertical periodicity was taken to be a 20 Å cell height. We used the 3-21g^* basis set. GAUSSIAN 03 applies a gradient-corrected correlation functional of Perdew, Burke, and Ernzerhof (PRE) method to account for the periodic boundary conditions. This approach was compared with optimization results using VASP. We used the GGA in our PBE computational model because it is the only approximation

available in our calculation for the CH_4 adsorbed on a single layer sheet of graphite. We first set the graphite parameters to experimental values $a=2.46$ Å then; both the CH_4 and the substrate are relaxed in this one layer case. In the optimization, all of the graphite x and y coordinates are changed by less than 0.01 Å, while the maximal height difference is in the molecule above the surface was only 0.056 Å. A multilayer model with a larger unit cell was well beyond the limits of our computer power. The G03 PBE method, taking the GGA for exchange correlation, gives the adsorption energy to be 147.378 meV at $\sqrt{3}\times\sqrt{3}$ coverage and one-layer graphite.

[1] L. W. Bruch, J. Chem. Phys. **87**, 5518 (1987).
[2] James M. Phillips, and M. D. Hammerbacher, Phys. Rev. B **29**, 5859 (1984).
[3] James M. Phillips, Phys. Rev. B **29**, 5865 (1984).
[4] James M. Phillips, Phys. Rev. B **34**, 2823 (1986).
[5] Kathleen A. Hunzicker, James M. Phillips, Phys. Rev. B **34**, 8843 (1986).
[6] James M. Phillips and Christopher D. Hruska, Phys. Rev. B **39**, 5425 (1989).
[7] A. Frisch *et al.*, GAUSSIAN 03, Gaussian, Inc., Pittsburgh, PA, 2003.
[8] Computer code VASP, 2003, http://cms.mpi.univie.ac.at/vasp/
[9] M. C. Payne, M. P. Teter, D. C. Allan, T. A. Arias, and J. D. Joannopoulos, Rev. Mod. Phys. **64**, 1045 (1992).
[10] G. Kresse and J. Hafner, Phys. Rev. B **47**, 558 (1993).
[11] G. Kresse and J. Furthmüller, Phys. Rev. B **54**, 11169 (1996).
[12] G. Kresse and D. Joubert, Phys. Rev. B **59**, 1758 (1999).
[13] P. E. Blöchl, Phys. Rev. B **50**, 17953 (1994).
[14] L. W. Bruch, M. W. Cole, and E. Zaremba, *Physical Adsorption: Forces and Phenomena* (Clarendon Press, Oxford, 1997).
[15] G. Vidali, G. Ihm, H-Y. Kim, and M. W. Cole, Surf. Sci. Rep. **12**, 133 (1991).
[16] J. G. Dash, *Films on Solid Surfaces* (Academic Press, New York, 1975).
[17] W. A. Steele, *The Interaction of Gases with Solid Surfaces* (Pergamon Press, New York, 1974).
[18] H. K. Kim, M. H. W. Chan, Phys. Rev. Lett. **53** 170 (1984).
[19] H. K. Kim, Q. M. Zhang, and M. H. W. Chan, Phys. Rev. B **34**, 4699 (1986).
[20] H. K. Kim, Q. M. Zhang, M. H. W. Chan, Phys. Rev. Lett. **56**, 1579 (1986).
[21] G. Constabaris, J. R. Sams, and G. D. Halsey, J. Phys. Chem. **65**, 367 (1961).
[22] M. S. Pettersen, M. J. Lysek, and D. L. Goodstein, Surf. Sci. **175**, 141 (1986).
[23] J. J. Hamilton and D. L. Goodstein Phys. Rev. B **28**, 3838 (1986).
[24] D. L. Goodstein, J. J. Hamilton, M. J. Lysek, and G. Vidali, Surf. Sci. **148**, 187 (1984).
[25] Sydney Ross, Jeffrey K. Saelens, and James P. Oliver, J. Phys. Chem. **66**, 696 (1962).
[26] Klaus Knorr, Phys. Rep. **214**, 113 (1992).
[27] J. Z. Larese and R. J. Rollefson, Surf. Sci. **127**, L172 (1983).
[28] J. Z. Larese and R. J. Rollefson, Phys. Rev. B **31**, 3048 (1985).
[29] J. W. Riehl and K. Koch, J. Chem. Phys. **57**, 2199 (1972).
[30] P. Vora, S. K. Sinha, and R. K. Crawford, Phys. Rev. Lett. **43**, 704 (1979).
[31] A. Glachant, J. P. Coulomb, M. Bienfait, C. Marti, and J. G. Dash, *Ordering in Two Dimensions* (North Holland, New York, 1980), p. 203.
[32] J. Z. Larese, M. Harada, L. Passell, J. Krim, and S. Satiji, Phys. Rev. B **37**, 4735 (1988).
[33] J. P. Coulomb, M. Bienfait, and P. Thorel, Phys. Rev. Lett. **42**, 733 (1979).
[34] J. P. Coulomb, M. Bienfait, and P. Thorel, J. Phys. (Paris) **42**, 293 (1981).
[35] R. P. Humes, M. V. Smalley, T. Rayment, and R. K. Thomas, Can. J. Chem. **66**, 557 (1988).
[36] M. W. Newbery, T. Rayment, M. V. Smalley, R. K. Thomas, and J. W. White, Chem. Phys. Lett. **59**, 461 (1978).
[37] M. V. Smalley, A. Hüller, R. K. Thomas, and J. W. White, Mol. Phys. **44**, 533 (1981).
[38] G. Bomchil, A. Huller, T. Rayment, S. J. Roser, M. V. Smalley, R. K. Thomas, and J. W. White, Philos. Trans. R. Soc. London, Ser. B **290**, 537 (1980).
[39] J. M. Gay, A. Dutheil, J. Krim, and Suzanne, Surf. Sci. **177**, 25 (1986).
[40] E. S. Severin and D. J. Tildesley, Mol. Phys. **41**, 1401 (1980).
[41] W. R. Hammond and S. D. Mahanti, Surf. Sci. **234**, 308 (1990).
[42] D. B. Litvin, Thin Solid Films **106**, 203 (1983).
[43] Kazuo Maki and Michael L. Klein, J. Chem. Phys. **74**, 1488 (1981).
[44] S. Jiang, C. L. Rhykerd, P. B. Balbuena, L. A. Pozhar, and K. E. Gubbins, in Proceedubgs if the Fourth International Conference on Fundamentals of Adsorption, 1992 (unpublished), p. 301.
[45] S. Jiang, K. E. Gubbins, and J. A. Zollweg, Mol. Phys. **80**, 103 (1993).
[46] G. Herzberg, *Molecular Spectra and Molecular Structure II* (Lancaster Press, Van Nostrand, New York, 1966).
[47] D. L. Gray and A. G. Robiette, Mol. Phys. **37**, 1901 (1979).
[48] S. E. Weber, S. Talapatra, C. Journet, A. Zambano, and A. D. Migone, Phys. Rev. B **61**, 13150 (2000).
[49] M. Muris, N. Dufan, M. Bienfait, N. Dupont-Pavlovsky, Y. Grillet, and J. P. Palmari, Langmuir **16**, 7019 (2000).
[50] S. Talapatra and A. D. Migone, Phys. Rev. B **65**, 045416 (2002).
[51] P. Giannozzi, R. Car, and G. Scoles, J. Chem. Phys. **118**, 1003 (2003).
[52] Xianwei Sha and Bret Jackson, Surf. Sci. **496**, 318 (2002).
[53] Xianwei Sha, Bret Jackson, and Didier Lemoine, J. Chem. Phys. **116**, 7158 (2002).
[54] G. Kresse and J. Furthmüller, Comput. Mater. Sci. **6**, 15 (1996).
[55] J. K. Kjems, L. Passell, H. Taub, J. G. Dash, and A. D. Movaco, Phys. Rev. B **13**, 1446 (1976).
[56] H. P. Schildberg and H. J. Lauter, Surf. Sci. **208**, 507 (1989).
[57] J. Furthmüller and J. Hafner, G. Kresse, Phys. Rev. B **50**, 15606 (1994), and references contained therein.
[58] J. M. Phillips, F. M. Leibsle, A. J. Holder, and T. Keith, Surf. Sci. **545**, 1 (2003).
[59] Paul S. Bagus and Francesc Illas, in *The Encyclopedia of Com-*

putational Chemistry (Wiley, New York, 1998), Vol. 4, p. 2870.
[60] M. Cinke, J. Li, W. Bauschlicher, Jr., A. Ricca, and M. Meyyappan, Chem. Phys. Lett. **376**, 761 (2003).
[61] Jijun Zhao, Alper Buldum, Jie Han, and Jian Ping Lu, Nanotechnology **13**, 195 (2002).
[62] Thomas Zecho, Andreas Güttler, Xianwei Sha, Bret Jackson, and Jürgen Küppers, J. Chem. Phys. **117**, 8486 (2002).
[63] Wai-Leung Yim, Oleg Byl, John T. Yates, Jr., and J. Karl Johnson, J. Chem. Phys. **120**, 5377 (2004).
[64] Kate Wright, Ian H. Hillier, Mark A. Vincent, and G. Kresse, J. Chem. Phys. **111**, 6942 (1999).
[65] R. C. Tatar, and S. Rabii, Phys. Rev. B **25**, 4126 (1982).
[66] R. Ahuja, S. Auluck, J. Trygg, J. M. Wills, O. Eriksson, and B. Johansson, Phys. Rev. B **51**, 4813 (1995).
[67] O. Dubay and G. Kresse, Phys. Rev. B **67**, 035401 (2003).
[68] D. Lamoen and B. N. J. Persson, J. Chem. Phys. **108**, 3332 (1998).
[69] Marek Gajdoš, Andreas Eichler, and Jürgen Hafner, J. Chem. Phys. **16**, 1141 (2004).
[70] F. Tuinstra and J. L. Koenig, J. Chem. Phys. **53**, 1126 (1970).
[71] S. Y. Leung, M. S. Dresselhaus, and G. Dresselhaus, Physica B & C **105**, 375 (1981).
[72] J. L. F. Da Silva, C. Stampfl, and M. Scheffler, Phys. Rev. B **72**, 075424 (2005).
[73] Paul S. Bagus (private communication).